

## EFFECT OF MALEIC ANHYDRIDE ON KENAF DUST FILLED POLYCAPROLACTONE/THERMOPLASTIC SAGO STARCH COMPOSITES

Siang Yee Chang,<sup>a,\*</sup> Hanafi Ismail,<sup>b</sup> and Qumrul Ahsan<sup>a</sup>

The utilization of biodegradable polymers for various applications has been restricted mainly by its high cost. This report aims to study the water absorption and mechanical properties of kenaf dust-filled polycaprolactone/thermoplastic sago starch biodegradable composites as a function of filler loading and treatment with maleic anhydride. While water absorption in untreated biocomposites increased as a function of filler loading, treated biocomposites resulted in weight loss, whereby low molecular weight substances were dissolved into the aging medium. The kenaf dust imparts reinforcing effects on the biocomposites, resulting in improved mechanical properties. This is further attested by morphological studies in which kenaf dust was well dispersed in the polycaprolactone/thermoplastic sago starch blend matrix. The addition of maleic anhydride into the polycaprolactone/thermoplastic sago starch blend resulted in a homogeneous mixture. At low filler loading, strain at break of the maleated polycaprolactone/thermoplastic sago starch blend increased at the expense of tensile strength and modulus. This is most likely due to the excessive dicumyl peroxide content, which caused chain scission of the polycaprolactone backbone. Tensile strength and modulus improved only when high filler loading was employed.

*Keywords:* Kenaf fiber; Thermoplastic sago starch; Polycaprolactone; Biocomposites; Maleic anhydride; Processability; Mechanical properties; Water absorption; Morphology

*Contact information:* a: Department of Engineering Materials, Faculty of Manufacturing Engineering, Universiti Teknikal Malaysia Melaka, Ayer Keroh, Melaka, 75450 Malaysia; b: Department of Polymer Engineering, School of Materials & Mineral Resources Engineering, Universiti Sains Malaysia, Nibong Tebal, Pulau Pinang, 14300 Malaysia; \* Corresponding author: changsy@utem.edu.my

### INTRODUCTION

The ever-growing environmental pressure caused by the huge-scale accumulation of plastic waste has spurred a thrust into the development of biodegradable or environmentally acceptable materials (Gáspár et al. 2005; Bogoeva-Gaceva et al. 2007). These biodegradable materials can be completely degraded into natural ecosystems, such as active sludge, natural soil, lake, and marine environments. Accordingly, the biodegradability of biodegradable materials corresponds to the ability to be chemically transformed by the action of biological enzymes or microorganisms such as bacteria, fungi, and algae to biomass and biological by-products (Wu 2003; di Franco et al. 2004; Kim et al. 2006; Rosa et al. 2009). Also, their chemical chains may be broken down by nonenzymatic processes such as chemical hydrolysis (Gross and Kalra 2002). This process can be considered as a biologically mediated recycling of plastic items (di Franco

et al. 2004). A large number of biodegradable polymers are commercially available, ranging from agro-polymers such as starch and protein, poly(hydroxyl butyrate) (PHB), poly(lactic acid) (PLA), polycaprolactone (PCL), polyesteramide (PEA), etc. Although these biodegradable polymers can partially solve the problem of non-biodegradable plastic waste pollution, the majority of biodegradable polymers are not widely used because they are too expensive, and the range of the material selection suitable for various end-use products is limited (John et al. 1998; Kim et al. 2006; Bogoeva-Gaceva et al. 2007; Hong et al. 2009).

To circumvent the problems of utilizing biodegradable polymers, polymer blending is an alternative to provide a potential route towards more economic, fully biodegradable materials. Thus, in this study, the blend of PCL with thermoplastic starch (PCL/TPS) was used as matrix. In order to impart additional advantages of improving physical and mechanical properties to the biopolymer blend, cellulosic fibers were incorporated into the biodegradable matrix to produce biocomposites, which are quite similar to the already known synthetic fiber-reinforced polymers (di Franco et al. 2004). Fiber-reinforced biocomposites will increase the use of this blend and its application into various areas such as automotive and packaging products (Bledzki and Gassan 1999). This is because the composites can withstand higher stresses than either of their individual constituents in such a way that the fibers and matrix interact and redistribute the stresses (Abu-Sharkh and Hamid 2004). Recently, kenaf has been gaining a lot of attention as a biomass-based additive due to its high modulus of 60 GPa as a result of its high cellulose content (about 72.8 wt %) (Liu et al. 2007).

Despite being a very interesting integration with many potential applications and environmental benefits, like other composites, the properties of kenaf-filled PCL/TPS biocomposites are handicapped by several important problems, namely, the lack of proper interfacial adhesion, poor resistance to moisture absorption, and low dimensional stability (Lee et al. 2009). While PCL is essentially hydrophobic in nature, both TPS and kenaf are highly susceptible to moisture absorption due to the presence of polar groups. Even though both TPS and kenaf have polar groups such as hydroxyl and carboxyl groups that can have some physical interactions during processing, these physical interactions are limited and typically do not lead to significant improvements in performance (Liu et al. 2005).

The strength of fiber/matrix interfacial adhesion is essential for stress transfer between the two constituents (Abu-Sharkh and Hamid 2004; Cyras et al. 2002). Over the past few decades, many approaches towards enhancing the fiber/matrix interaction degree have been pursued through fiber surface modification to facilitate fiber dispersion and induce bond formation between the fiber and matrix. This is achieved through either a chemical or physical modification route (Bledzki and Gassan 1999; George et al. 2001; Sreekala et al. 2000; Mohanty et al. 2005).

In this study, an attempt is made to produce biocomposites from a PCL-thermoplastic sago starch (TPSS) blend and kenaf dust (KD) at various filler loading in order to investigate the effect of maleic anhydride (MAH) addition on the mechanical properties and water absorption of the PCL/TPSS/KD biocomposites.

## EXPERIMENTAL

### Materials

Polycaprolactone grade H5 ( $M_w = 50,000$ ,  $T_m = 60^\circ\text{C}$ ) was supplied by Daicel Chemical Industries Ltd., Japan, while the sago starch was obtained from the Land Custody Development Authority Sarawak (LCDA), Malaysia. The starch has granular size ranges from 9 to 35  $\mu\text{m}$  and decomposes at  $230^\circ\text{C}$ . Raw kenaf fiber used in this study was supplied by the Forest Research Institute Malaysia (FRIM). The fiber was extracted from the core of a mature kenaf plant's (*Hibiscus cannabinus*) stem, and was subjected to grinding process to form fiber dust before being used as filler in the subsequent composite fabrication. The ground fiber has a diameter less than 250  $\mu\text{m}$ . Meanwhile, maleic anhydride (MAH) and dicumyl peroxide (Luperox® DCP) used were supplied by Sigma-Aldrich (M) Sdn. Bhd.

### Methods

#### *Preparation of thermoplastic sago starch (TPSS)*

The sago starch powder was dried in a vacuum oven (EV 018 nüve, Turkey) for 24 hours at  $80^\circ\text{C}$ , followed by mixing it with 35 wt% glycerol in a beaker by using a glass rod. The compound was subsequently subjected to equilibration for 24 hours at room temperature in desiccators. To facilitate the formation of TPSS, the compound was rolled at  $150^\circ\text{C}$  for 10 minutes by using a heated two-roll mill (Labortex Co. Ltd., Taiwan) and later granulated.

#### *Preparation of uncompatibilized and compatibilized PCL/TPSS blend*

PCL pellets were dried in an oven at  $40^\circ\text{C}$  for 24 hours prior to processing. Later, the PCL pellets and granulated TPSS were mixed together in a weight ratio of 1:1. This melt-mixing was performed at  $90^\circ\text{C}$  with a rotor speed of 35 rpm for 10 minutes using an internal mixer (Thermo Haake Rheomix Polydrive R600/610, USA). For the uncompatibilized blend, the PCL pellets were charged into the mixing chamber initially and followed by the TPSS at the third minute (min-3). The process was then continued for another seven minutes.

As for the compatibilized blend, 4.5 phr MAH solid crystals were added at the next minute after PCL was loaded into the internal mixer and followed by 0.5 phr DCP at the min-2. Subsequently, TPSS was inserted at the min-3. The grafted product was discharged from the mixing chamber and granulated after 10 minutes of melt-mixing.

#### *Preparation of kenaf dust filled PCL/TPSS biocomposites*

Prior to composite fabrication, the kenaf dust was dried in a vacuum oven at  $80^\circ\text{C}$  for 24 hours. Melt-mixing of PCL/TPSS blend with kenaf dust was conducted at  $90^\circ\text{C}$  for 10 minutes with a rotor speed of 35 rpm to form the composite compound. The kenaf dust loading was varied between 0 (control) to 30 phr (See Table 1). The PCL/TPSS blend was initially preheated for 3 minutes and followed by the addition of kenaf dust within the subsequent 30 seconds. The composite compounding process lasted for 10 minutes. On-going torque measurements were taken throughout the melt-mixing process to indicate the incorporation of fillers into the matrix and its uniformity.

**Table 1.** Description of Composition of PCL/TPSS/KD Biocomposites and Relative Codes

Code	PCL (phr)	TPSS (phr)	KD (phr)	MAH (phr)	DCP (phr)
PCL/TPSS (control)	50	50	-	-	-
PCL/TPSS/5KD	50	50	5	-	-
PCL/TPSS/10KD	50	50	10	-	-
PCL/TPSS/15KD	50	50	15	-	-
PCL/TPSS/30KD	50	50	30	-	-
PCL-MAH/TPSS/5KD	50	50	5	4.5	0.5
PCL-MAH/TPSS/10KD	50	50	10	4.5	0.5
PCL-MAH/TPSS/15KD	50	50	15	4.5	0.5
PCL-MAH/TPSS/30KD	50	50	30	4.5	0.5

*Compression molding*

The PCL/TPSS/KD composites were then subjected to compression molding in an electrical heated hydraulic press (KaoTieh GoTech Testing Machine Inc., Taiwan). Hot press procedures involved preheating for 10 minutes and followed by compression under 10 MPa for 2 minutes at 160°C (Shin et al. 2004). This is to ensure flowability of the KD in the PCL/TPSS blend within the mold to form 1 mm-thick sheets. Even though PCL melts at approximately 60°C, the fluidity of the PCL/TPS blend is as low as 0.18±0.03 g/10 min due to the presence of plasticized starch (Rosa et al. 2004). Besides, it is found that the PCL only begins to degrade upon 350°C (Di Franco et al. 2004). All pressed sheets (150 × 150 × 1 mm) were later cold-pressed for 5 minutes at room temperature.

*Tensile test*

The tensile test was carried out with a universal testing machine Instron 3366 (Instron, USA) according to ASTM D638. A crosshead speed of 5 mm/min was used, and the test was performed at 25 ± 3°C. The specimens in strip form (115.0 × 12.2 × 1.0 mm) were cut from the compression molded sheets with a die cutter and tested for tensile strength, elongation at break, and Young's modulus.

*Water absorption study*

The water absorption test was performed following the ASTM D570-81 method with the strip form test piece similar to that of tensile specimen. The samples were dried in an oven at 40°C for 24 hours, cooled in a desiccator at room temperature, and then immediately weighed to the nearest 0.0001 g (this weight was designated as  $M_o$ ). Thereafter, the conditioned samples were immersed in distilled water and maintained at room temperature for a test period of two months. The measurements were taken at every 24 hours interval for the first week and later reduced to a weekly measurement. During the mass measurement, the samples were removed from the water, gently blotted with cloth and tissue paper to remove excess water on the surface, immediately weighed to the nearest 0.0001 g (designated as  $M_i$ ), and returned to the water. Three samples were used to evaluate the average water absorption behavior of each compound. The percentage of water absorption was regarded as percentage of weight gain and was calculated to the nearest 0.01% using the equation 1 as follows:

$$\text{Weight gain, } M_w (\%) = [(M_i - M_o) / M_o] \times 100\% \quad (1)$$

where  $M_w$  is the percentage of weight gain of the tested samples,  $M_o$  is the original weight of the samples prior to immersion, and  $M_i$  refers to the weight of the samples after immersion at a designated time.

#### *Morphological study*

Morphology of the composites was examined through observation under a Field Emission Scanning Electron Microscopy (Zeiss Supra 35VP, Germany) operating at 10 kV. The specimens were placed on the sample holder by mounting with double-sided carbon tape. Since the specimens were non-conductive, they were sputtered with gold (thickness of 10 nm) on Polaron SC 515 sputter coater. The observation was conducted to study the morphology of fracture surface of the specimens after the tensile test.

#### *Fourier Transform Infrared analysis*

Fourier Transform Infrared (FTIR) analysis was carried out using the Attenuated Total Reflectance (ATR) technique on Fourier Transform Infrared Spectroscopy (Perkin Elmer System 2000, USA). The samples were placed on top of the ATR crystal surface at a very intimate contact and the spectra were recorded in reflectance. All the spectra were recorded in the range of 4000 to 550  $\text{cm}^{-1}$ , with a resolution of 4  $\text{cm}^{-1}$  after 16 repetitions of scanning.

## RESULTS AND DISCUSSION

### **Grafting Mechanism of Polycaprolactone/Thermoplastic Sago Starch Blend**

In order to compatibilize hydrophobic PCL and hydrophilic TPSS, as well as increase the starch composition in the blend, MAH was grafted onto the PCL backbone through in-situ grafting in an internal mixer, using DCP as an initiator. When molten PCL is sheared in the presence of MAH and DCP at 90°C in an internal mixer, a series of reactions occurred, as illustrated in Fig. 1(a). The grafting reaction begins with thermal decomposition of DCP to form  $\text{RO}\cdot$  radical. This is followed by hydrogen abstraction of the  $\alpha$ -carbon atom relative to the ester carbonyl group and results in the formation of a PCL macromolecular radical. Subsequently, MAH is added to the PCL macromolecular radical, leading to the formation of PCL-MAH $\cdot$  radical, which later undergoes hydrogen transfer. The final graft structure formed through the in-situ grafting is PCL-MAH. The source for hydrogen might result from any MAH, PCL, or free radical available in the melt (Mani et al. 1999; Semba et al. 2006). In the subsequent compounding process with TPSS, the PCL-MAH undergoes hydrolysis so as to form hydrogen bonding with starch (Rahmat et al. 2009). In further compounding with KD, a hydrogen bond is formed between the PCL-MAH/TPSS and the hydroxyl group of KD, as shown in Fig. 1(b).

#### *Fourier transform infrared spectroscopy (FTIR)*

Figure 2 shows the FTIR spectra of PCL/TPSS and PCL-MAH/TPSS. The characteristic peaks of MAH that is grafted onto PCL are hardly identified, simply because both PCL and MAH possess a carbonyl  $\text{C}=\text{O}$  group. A similar problem has also been reported by Avella et al. (2000) and Raquez et al. (2008).

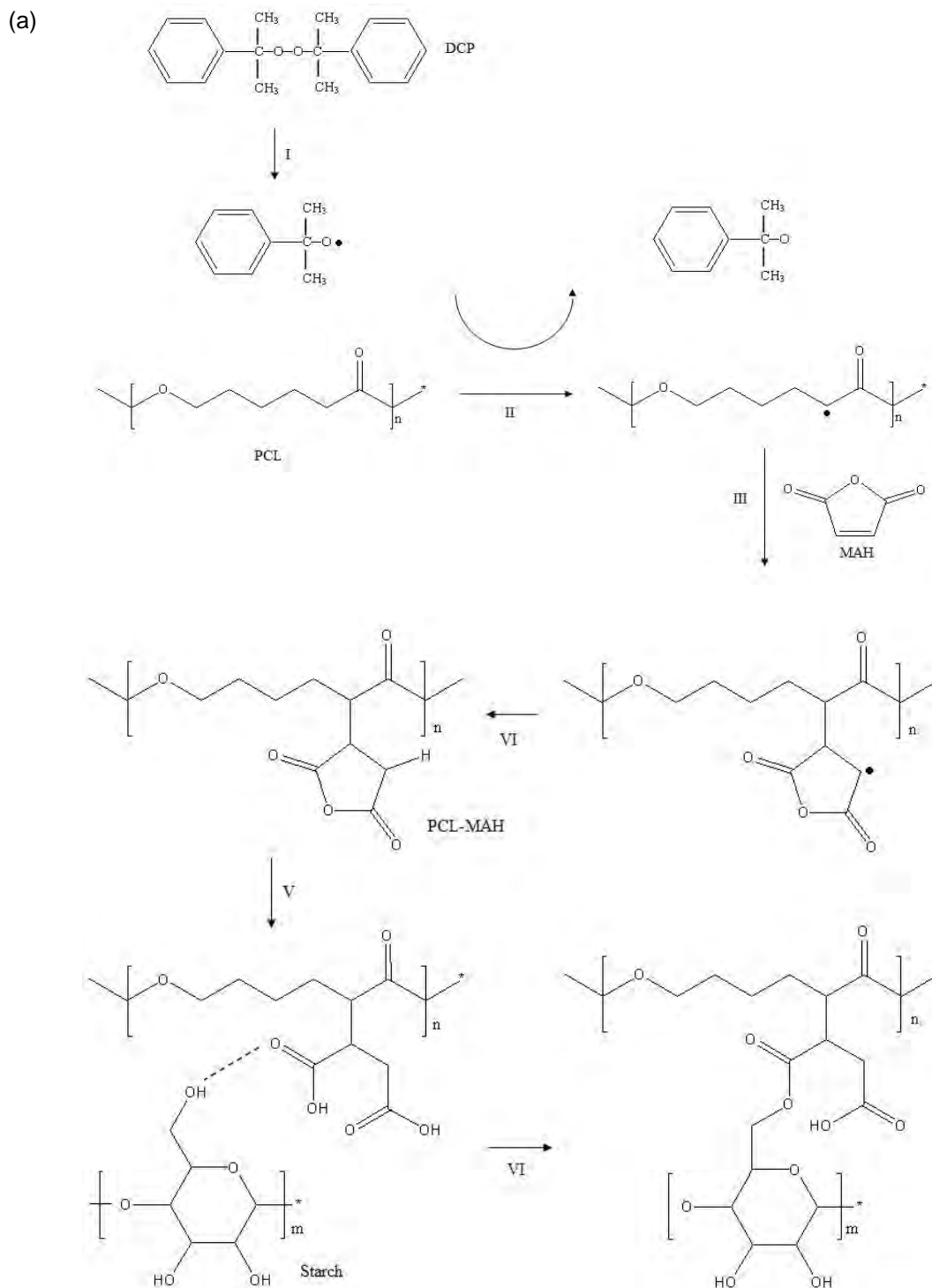


**Fig. 1a.** Reaction of maleic anhydride in PCL and TPSS (Raquez et al. 2008; Ramarad 2008; Rahmat et al. 2009)

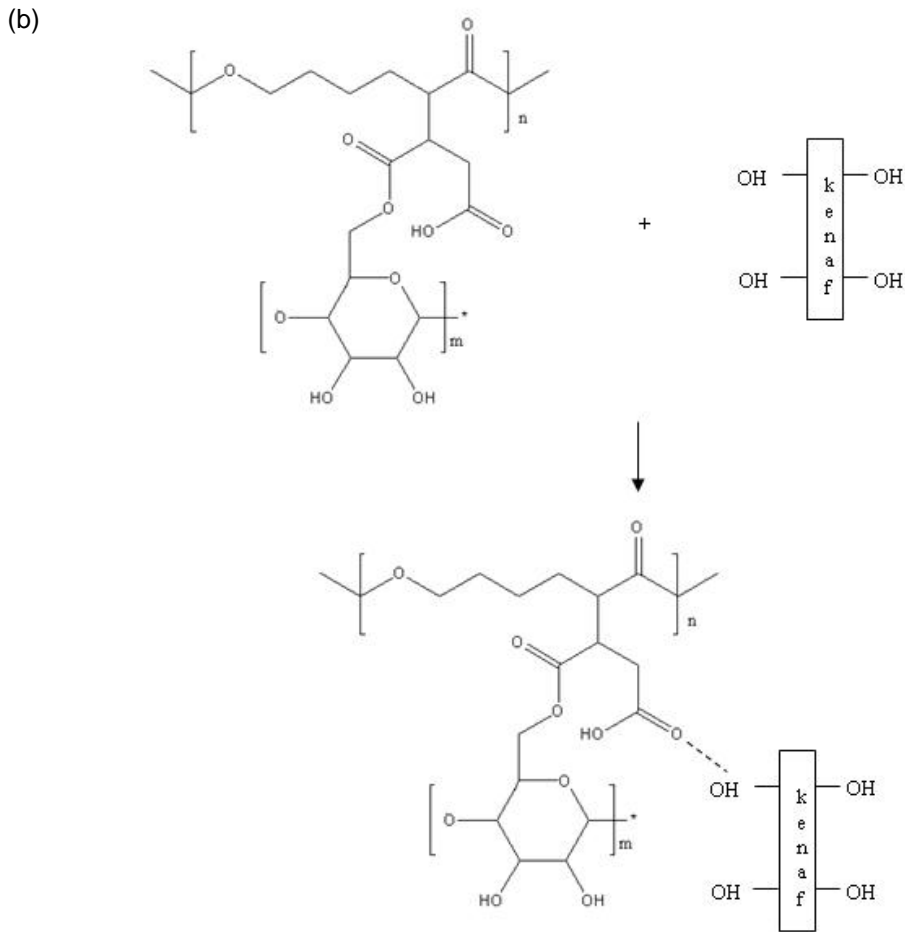


**Fig. 1b.** Proposed interaction between PCL-MAH/TPSS and KD

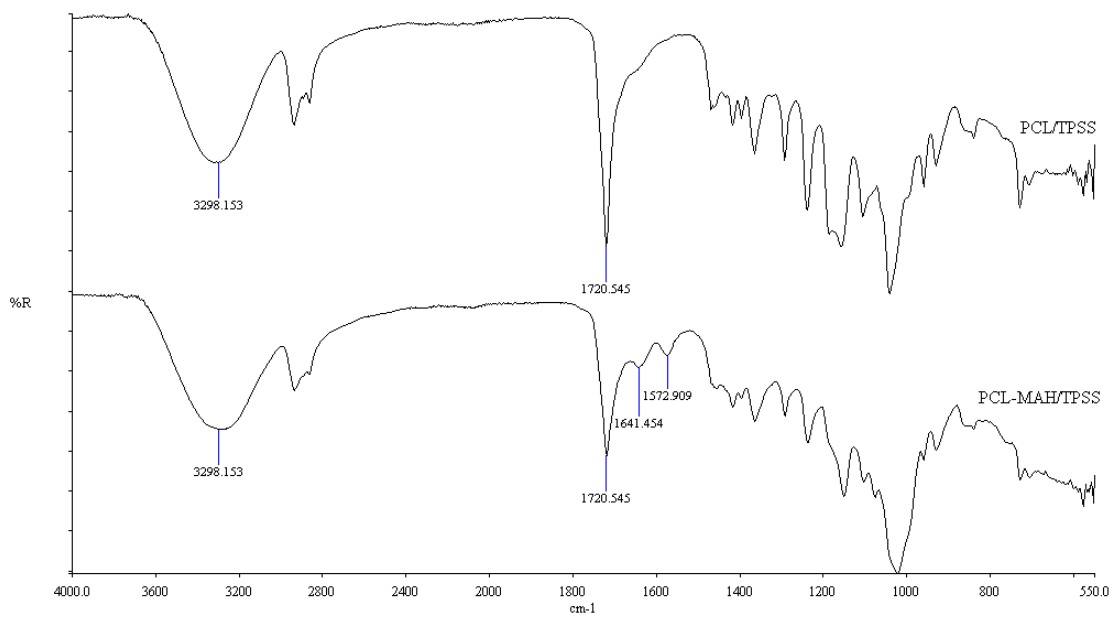


**Fig. 2.** Comparison of FTIR spectra between PCL/TPSS and PCL-MAH/TPSS

The characteristic peaks of MAH at 1739 and 1858  $\text{cm}^{-1}$  are associated with symmetric and asymmetric C=O stretching, respectively (Qiu et al. 2005). Both peaks are not observed in the FTIR spectra of PCL-MAH/TPSS because of overlapping of a very intense ester band of PCL at 1720  $\text{cm}^{-1}$ . However, Raquez et al. (2008) suggested that this may be because the MAH ring is fully reacted and opened, resulting in the appearance of additional peaks around 1550 to 1600  $\text{cm}^{-1}$ . Peaks at 1570  $\text{cm}^{-1}$  are assigned to the maleic substituent carboxylic groups (Berkovich et al. 1983). Meanwhile, the peak at 1640  $\text{cm}^{-1}$  which is attributed to the aliphatic alcohol group, most likely implies the presence of residual DCP.

### Processability

Figure 3 depicts the Haake mixing torque profiles of PCL/TPSS blend and its composites having various KD loading. In all cases, an initial loading peak was registered immediately upon the commencement of rotors and initial charging of solid materials into the mixing chamber, which in this case is the PCL/TPSS blend. The instant increase in torque can be attributed to high shear force required to rotate the rotors in the presence of PCL/TPSS blend prior to melting (Othman et al. 2006). It is noticeable that the virgin PCL/TPSS blend marked the highest loading torque of 22.4 Nm, while in the case of PCL/TPSS/KD biocomposites, the loading peaks decreased with the increase of filler loading due to the reduction of charged weight of PCL/TPSS blend into the mixing chamber. In other words, the torque of the loading peak is dependent on the charged amount of PCL/TPSS blend. In all cases, shortly after loading, the PCL/TPSS blend started to melt under shear and high stock temperature, which is higher than the set temperature because of dispersion friction (Lei et al. 2007), resulting in reduction of the melt viscosity. The reduction in the melt viscosity is reflected by the sudden drop of the torque immediately after the loading peak as well as subsequent gradual decrease of the torque (Premalal et al. 2002). After 3 minutes of shearing, the PCL/TPSS blend shows almost stable torque and indicates completion of melting with an evidence of almost constant viscosity at fixed mixing conditions.

In biocomposites, a sudden increase of torque was again observed during the incorporation of KD into the molten PCL/TPSS blend at min-3. This is because the addition of KD filler into the melt has restricted the mobility of the macromolecule chains of PCL/TPSS, leading to an instant rise of viscosity of the melt. At this point, the torque value of the second peak is dependent on the filler loading (Kunanopparat et al. 2008). As the increase in filler loading accompanies a decrease in the matrix blend, the degree of resistance to deformability of the matrix blend also increases. This increase in resistance leads to high torque peaks of composites with higher filler loading. Once the fillers are well-wetted and well-dispersed in the polymer blend, the mixture becomes more homogeneous, and torque decreases gradually to a stable value. This stabilized torque value is termed the stabilization torque, which is an indicator of homogenization of filler in the melt (Demir et al. 2006). The measure of stabilization torque is taken as the average value between the 8<sup>th</sup> and 10<sup>th</sup> min of mixing. When the stabilization torque values are compared, it is clearly seen that a gradual rise in the values is observed as the filler loading increases.

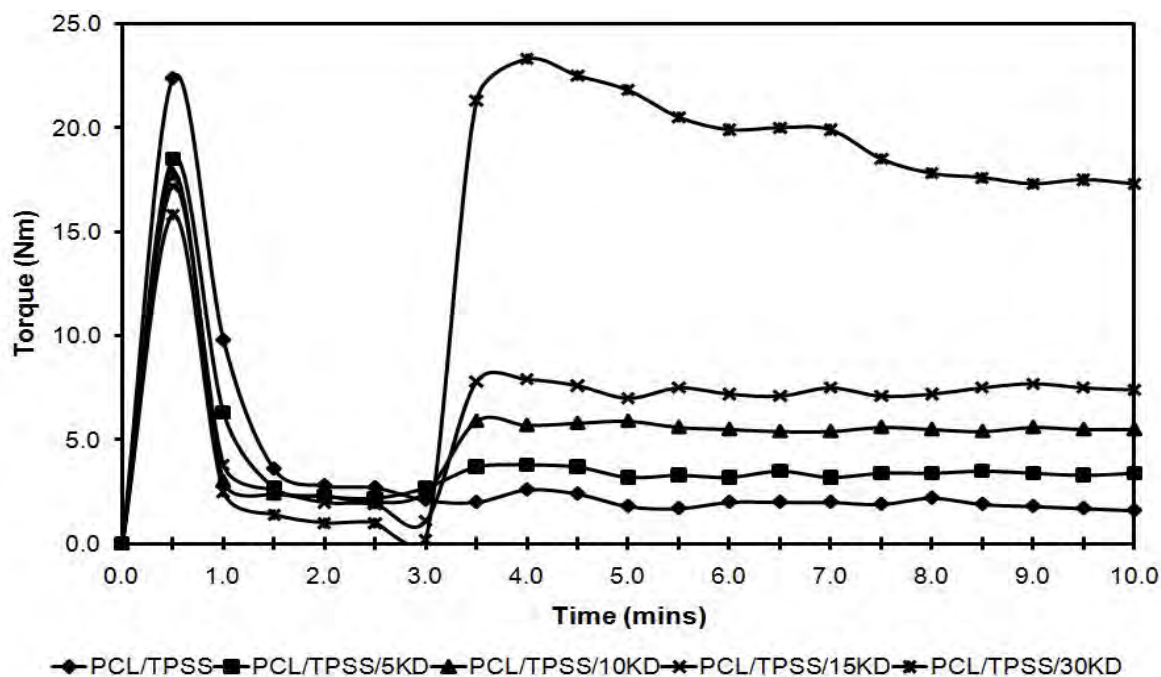


Fig. 3. Processing torque of PCL/TPSS/KD biocomposites versus time at different filler loading

While the overall mixing torque profile of the MAH-treated systems exhibited a similar trend as the untreated one, the comparison of stabilization torque between the control and MAH-treated biocomposites is presented in Fig. 4. Clearly, at low filler loading, the addition of PCL-MAH/TPSS resulted in lower stabilization torque as compared to the control.

Wu (2003) suggested that the improved rheological behavior of PCL-MAH/TPSS/KD biocomposites can be attributed to the conformational change of the TPSS molecule due to the formation of an ester carbonyl functional group between the PCL-MAH and TPSS (Wu 2003).

Another possible reason could be that there was greater chain scission as a result of higher concentrations of initiator (DCP) being incorporated, thus leading to decreased viscosity of the biocomposites (Mani et al. 1999).

Additionally, Othman et al. (2006) proposed a lubricating effect of MAH-grafted copolymers that are capable of facilitating the processing of composites by improving flow properties. However, when the filler loading exceeded 10 phr, it was observed that the stabilization torque of PCL-MAH/TPSS/KD biocomposites was higher than that of the control system. It is anticipated that the interaction between PCL-MAH/TPSS blend and the KD most likely becomes pronounced, leading to improved interfacial adhesion and thereby imposes higher restriction to molecular motion of the macromolecules. Furthermore, the higher tensile strength of PCL-MAH/TPSS/KD biocomposites (discussed later) reflects stronger filler/matrix interfacial adhesion.

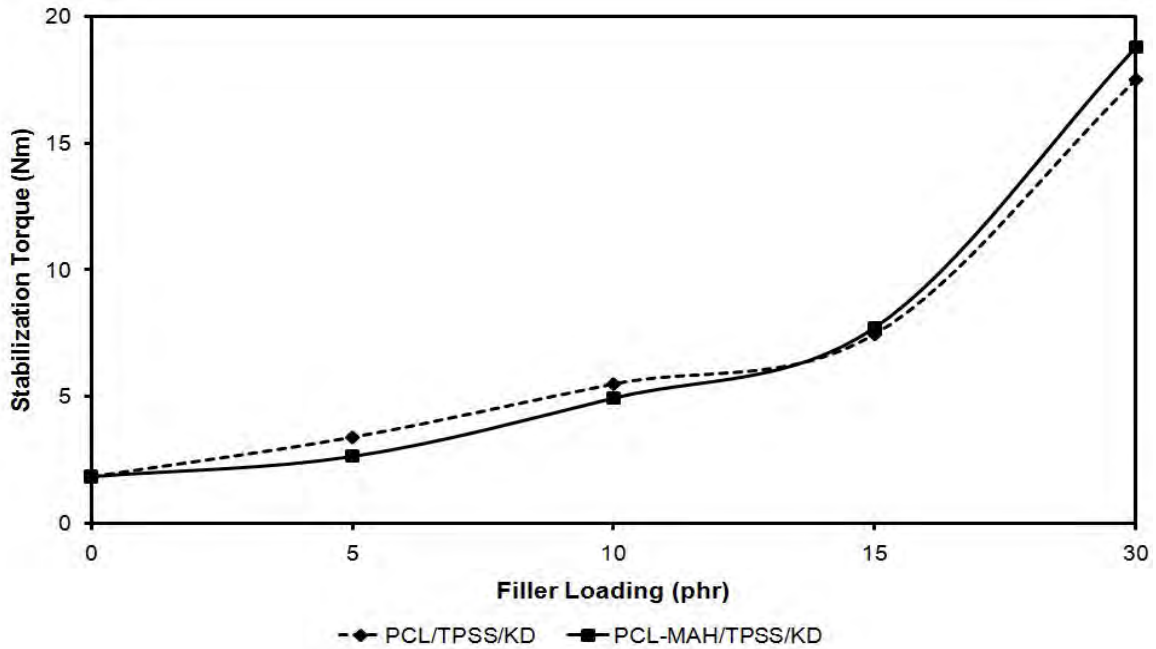


Fig. 4. Effect of maleic anhydride grafting on the stabilization torque of PCL/TPSS/KD biocomposites at different filler loading

**Water Absorption Behavior**

Typical water absorption curves with weight gain as a function of exposure time in water at room temperature for PCL/TPSS blend and its composites are shown in Fig. 5.

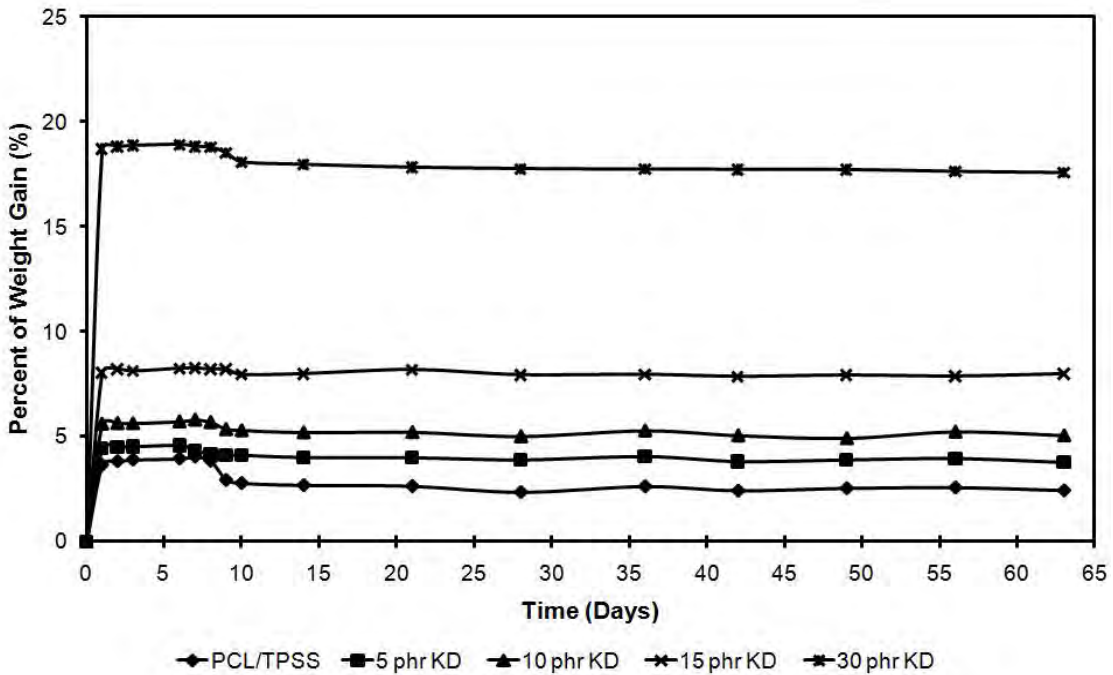
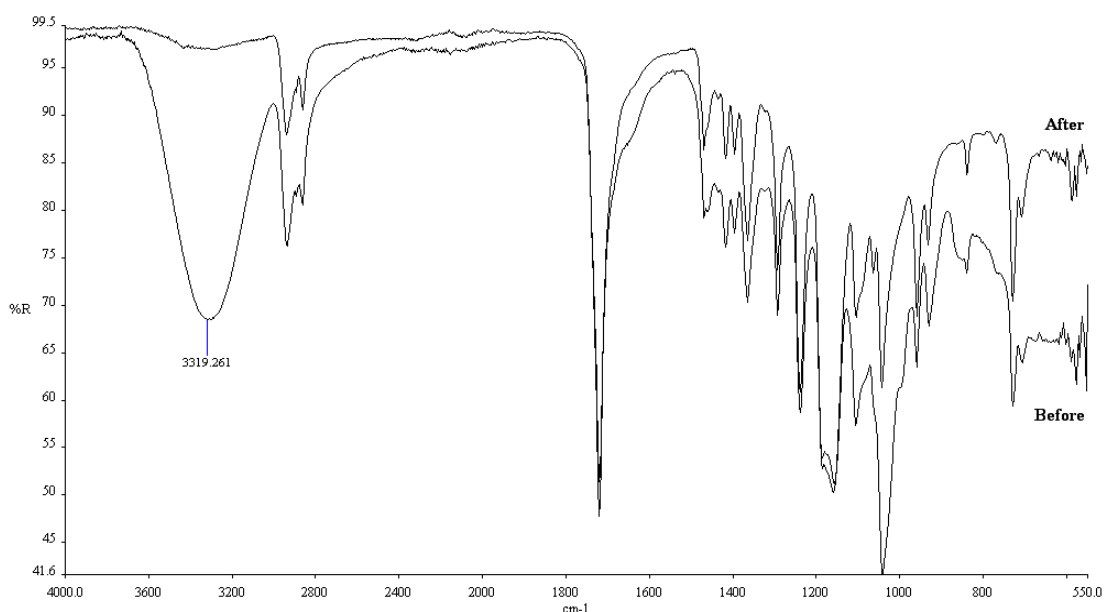


Fig. 5. Water absorption behavior of PCL/TPSS/KD biocomposites at different filler loading

In all cases, the water absorption process was sharp at the beginning and leveled off for some length of time where it approached equilibrium. Generally, for the PCL/TPSS/KD biocomposites, the water absorption at the equilibrium reached its maximum after 10 days of conditioning. It is noted that the PCL/TPSS blend had the lowest water absorption compared to its composites. While PCL is essentially hydrophobic (Sen and Bhattacharya 2000; di Franco et al. 2004; Rosa et al. 2005; Pan et al. 2008; Rahmat et al. 2009; Islam et al. 2009; Li and Favis 2010), only TPSS is responsible for taking up water in the PCL/TPSS blend, whereas the incorporation of KD in the biocomposites would further supplement the water absorption capacity. On top of that, the water absorption of the biocomposites increased with increasing filler loading. This can be rendered by two factors, which are (i) hydrophilicity of kenaf and (ii) the presence of voids between the matrix and filler. It is well known that the free hydroxyl groups on kenaf promote water absorptivity by forming hydrogen bonding with the water molecules, leading to increased water uptake with increasing filler loading

Besides, poor adhesion at the filler/matrix interfacial causes cracks and voids between the PCL/TPSS matrix and kenaf filler. This results in easy penetration and storage of water through the voids (Demir et al. 2006). Furthermore, it is supposed that at high filler loading, more water can fill in the voids that existed. Additionally, a close observation on the water absorption curves after 1 week revealed a slight decrease in sample mass for both PCL/TPSS blend and its composites. This was mainly due to the leaching out of some TPSS from the sample surface, which has been confirmed by the FTIR profiles of the biocomposites containing 0 phr KD, as illustrated in Fig. 6. A peak around  $3300\text{ cm}^{-1}$  which is associated with the hydroxyl group of starch (Raquez et al. 2008), had disappeared after the water absorption test. Hence, this further affirms that starch leached out due to its affinity to water. This is similar to that reported by John et al. (1997).



**Fig. 6.** FTIR spectra of PCL/TPSS blend before and after water absorption test

Figure 7 shows the effect of maleic anhydride addition on the water absorption behavior of PCL/TPSS/KD biocomposites. In contrast to the untreated system, there was significant weight loss in the MAH-treated samples after being immersed in water, rather than weight gain. Essentially, in the water absorption test, as explained earlier, the sample's weight gain is associated with the hydrophilic nature of kenaf and starch molecules, while the leaching out of glycerol, starch molecules, and low molecular weight substances is responsible for the sample's weight loss. Therefore, the total quantity of water absorbed by the sample at equilibrium reflected the maximal difference between the water uptake and material loss (Kunanopparat et al. 2008).

In the treated systems, it can be deduced that the effect of material leaching out is more significant than that of water uptake by the biocomposites. The decrease in water absorption capacity of the treated biocomposites is due to the enhanced adhesion between the filler and matrix through compatibilization grafting, which led to decrease of voids between the filler/matrix interfaces. This is evidenced from the morphological difference between untreated and treated biocomposites, as shown in Fig. 10 (c) and 11 (a), respectively. The reduction in the volume of voids rendered by the improved interfacial adhesion has, as a consequence, restricted water penetration or storage at the interface (Demir et al. 2006). Furthermore, according to Demir et al. (2006), another reason that hampered the water uptake capacity in the biocomposites is the formation of hydrogen or covalent bonds of the PCL-MAH/TPSS with some of the free hydroxyl groups of cellulose (Fig. 1 (b)), resulting in improved water resistance of KD. As a result, the water resistivity of treated biocomposites was enhanced, confirming that the effect of starch loss to be more remarkably severe and therefore resulting in negative values for weight gain measurement upon the water absorption test.

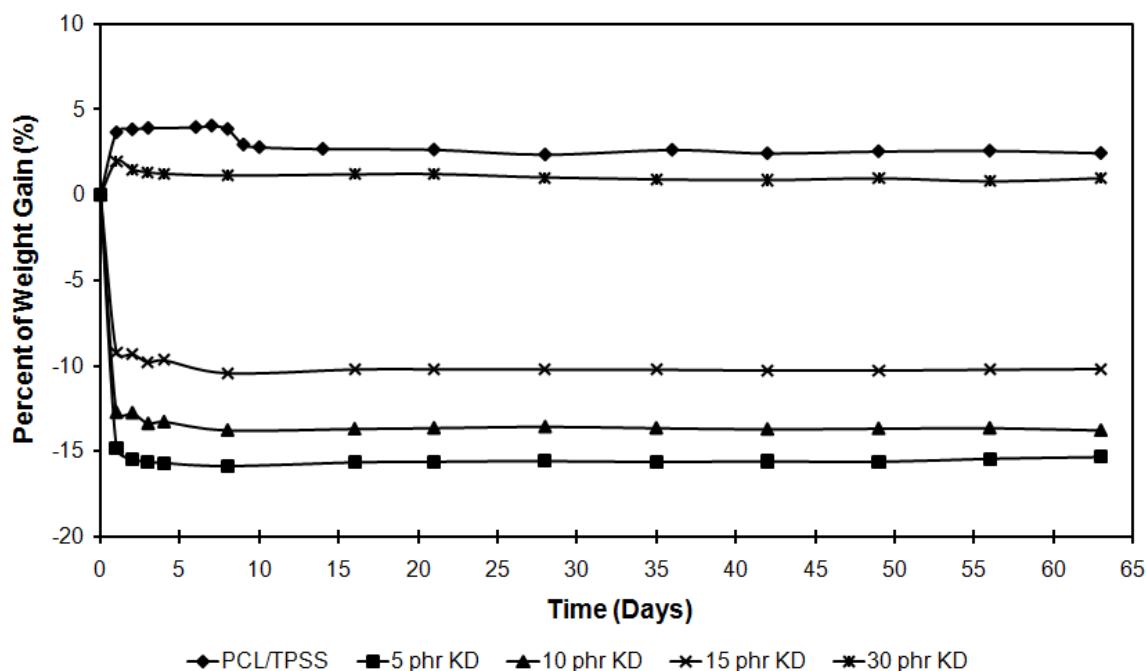


**Fig. 7.** Effect of maleic anhydride on water absorption behaviour of PCL/TPSS/KD biocomposites at different filler loading

Evidence of starch and low molecular weight substances (i.e. DCP) loss from the sample surface of treated biocomposites is manifested from FTIR results, as shown in Fig. 8, whereby the peak at 3300 and 1640  $\text{cm}^{-1}$  referring to the hydroxyl group of starch and DCP disappeared after immersion in water (Raquez et al. 2008). In terms of the effect of filler loading in this treated system, the amount of weight loss was reduced with increasing filler loading. This can be explained based on the fact that as more fillers are incorporated into the biocomposites, the content of possible starch loss is reduced yet accompanied by more water uptake by KD.

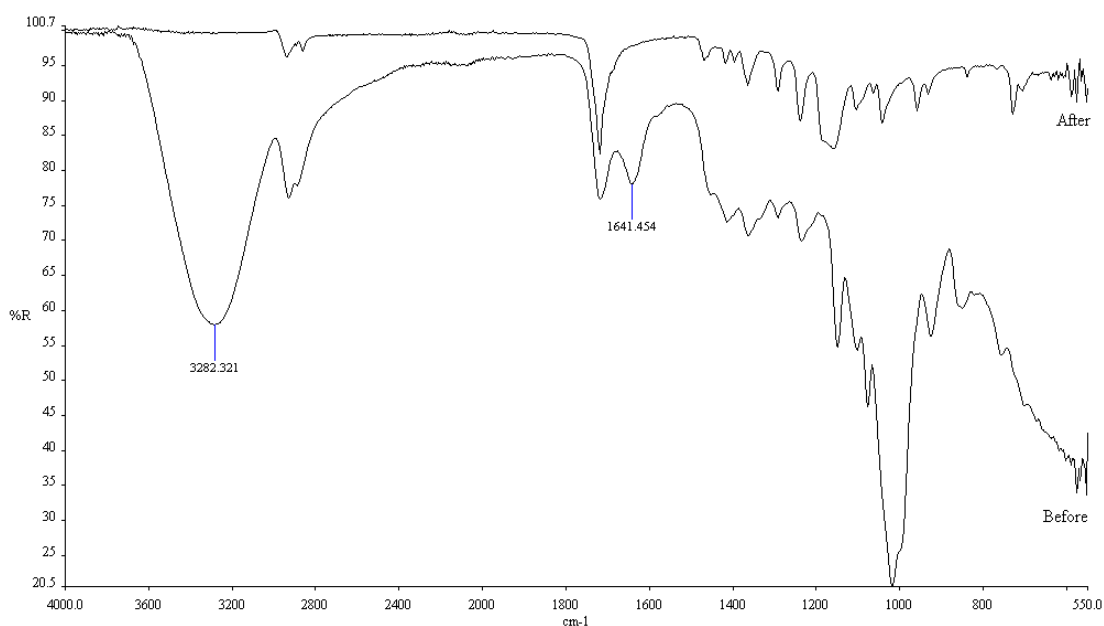


**Fig. 8.** FTIR spectra of PCL-MAH/TPSS/10KD biocomposites before and after water absorption test

### Mechanical Properties

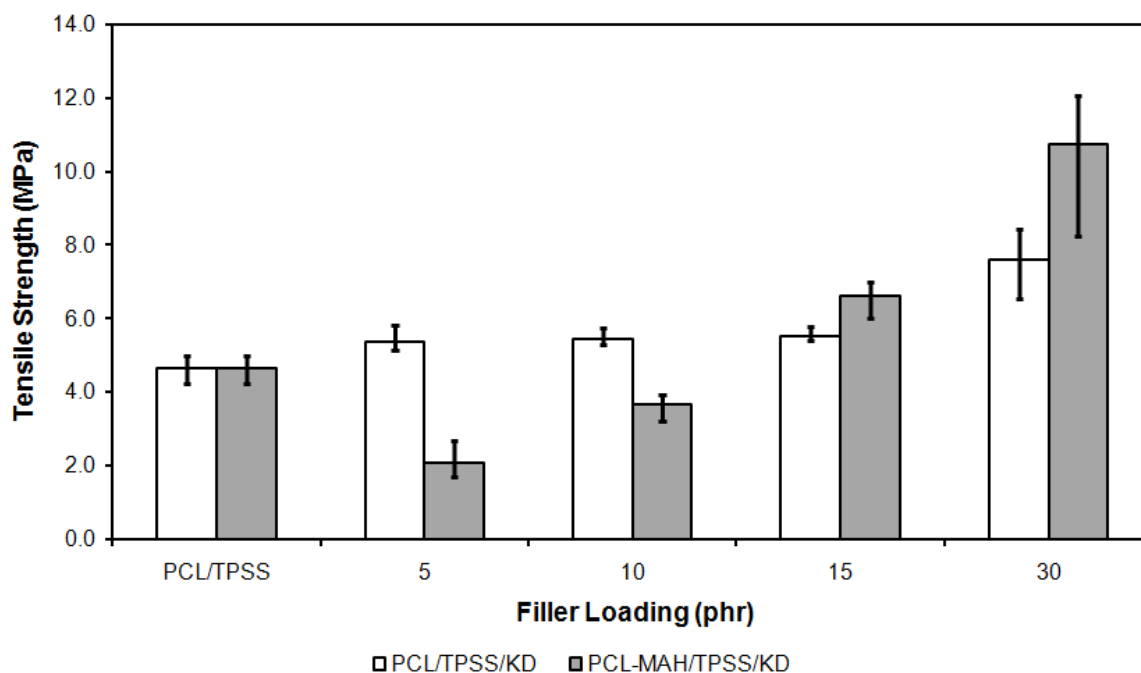
Table 2 shows the comparison of mechanical properties between the pristine PCL and PCL/TPSS blend from the literature and the present work. In this study, the control, untreated PCL/TPSS blend, exhibited a tensile strength of 4.65 MPa, an elongation at break of 5.31%, and a modulus of 192 MPa. It is noted that the control was of inferior in terms of tensile strength and elongation at break but with higher modulus as compared to the pristine condition. This is associated with the addition of 50 wt% TPSS, as supported by Avella et al. (2000) and Shin et al. (2004). The tensile fracture surface of the blend indicated that both PCL and TPSS are immiscible, forming distinguishable phases with the tendency of TPSS granules agglomeration, as illustrated in Fig. 10 (a). Agglomeration of TPSS granules was caused by the weak bonding between the PCL and TPSS, which results in low strength of the untreated PCL/TPSS blend. This is described by Pan et al. (2008), who noted that the agglomeration of kenaf creates regions of stress concentration in which less energy is needed for the crack propagation.

**Table 2.** Comparison of Mechanical Properties between the Pristine PCL and PCL/TPSS Blend

Amount of PCL	Amount of TPSS	Tensile Strength (MPa)	Young's Modulus (MPa)	Elongation at Break (%)	References
100 wt%	-	29	93	1090	Shin et al. 2004
100 wt%	-	33.0	280	1328	Avella et al. 2000
50 wt%	50 wt%	10	176	18	Shin et al. 2004
50 wt%	50 wt%	8.1	597	538	Avella et al. 2000
50 wt%	50 wt%	4.65	192	5.31	Present work

Figure 9, parts (a), (b), and (c) present the respective comparison of tensile strength, Young's modulus, and elongation at break of PCL/TPSS/KD and PCL-MAH/TPSS/KD biocomposites with various KD contents. Improvement in tensile strength is noted when KD was incorporated into the untreated PCL/TPSS blend, whereby the tensile strength reached up to 7.60 MPa at a filler loading of 30 phr. This can be explained by the fact that the filler is well-dispersed in the polymer blend, as illustrated in the fracture surface of untreated biocomposites in Fig. 10 (b)-(d). The good dispersion of the KD in the untreated biocomposites results in efficient stress transfer from the matrix to the filler (Pan et al. 2008). Thus, there is of every possibility that the KD imparted a reinforcing effect to the PCL/TPSS blend.

Although KD imparted reinforcing effect on the untreated PCL/TPSS blend, it is interesting to note that the improvement in the tensile strength of the untreated biocomposites became more significant at high filler loading (30 phr KD), while at low filler loading the effect was almost negligible and leveled off (Fig. 9 (a)).

**Fig. 9 (a).** Tensile strength of PCL/TPSS/KD and PCL-MAH/TPSS/KD biocomposites at different filler loading

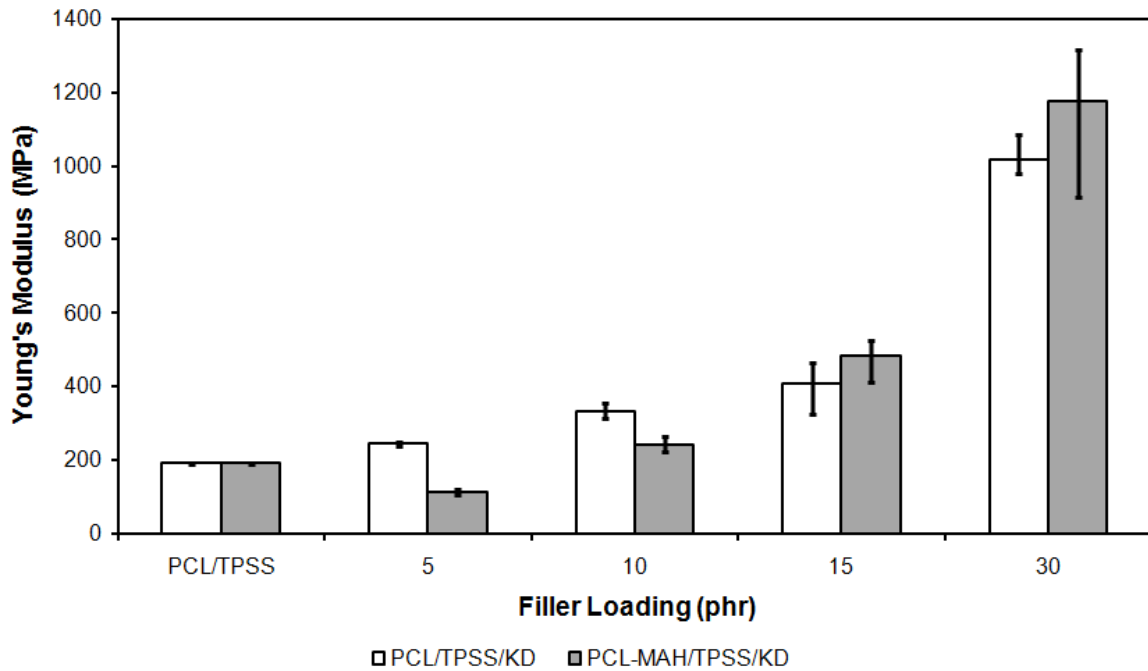


Fig. 9 (b). Young's modulus of PCL/TPSS/KD and PCL-MAH/TPSS/KD biocomposites at different filler loading

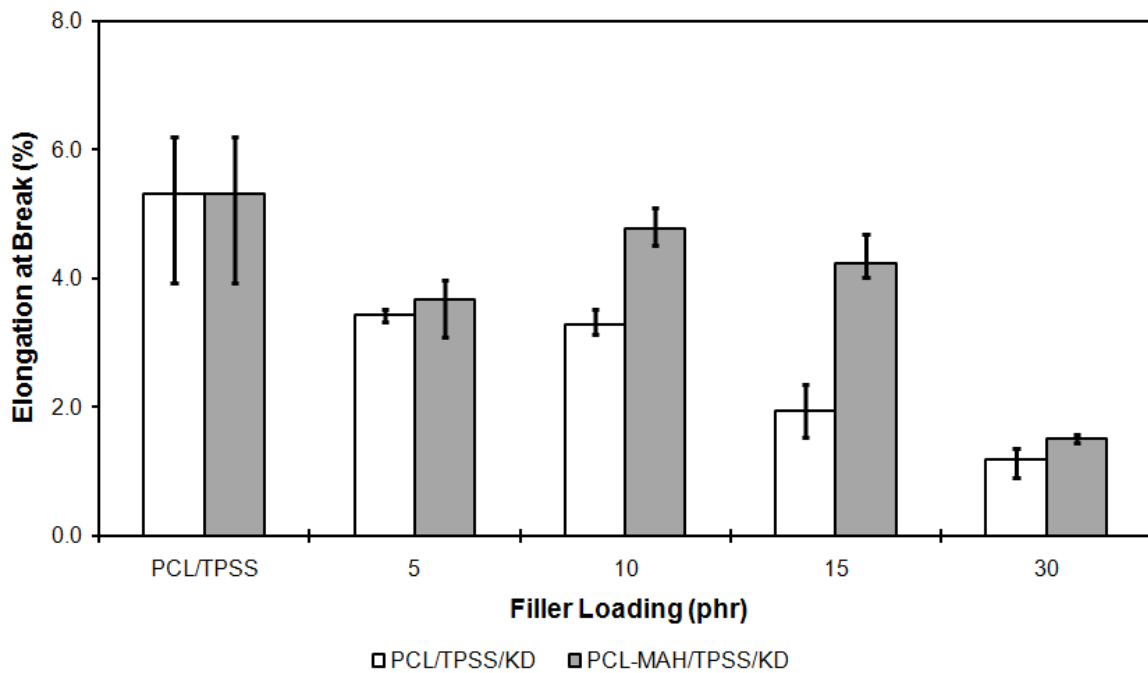


Fig. 9 (c). Elongation at break of PCL/TPSS/KD and PCL-MAH/TPSS/KD biocomposites at different filler loading

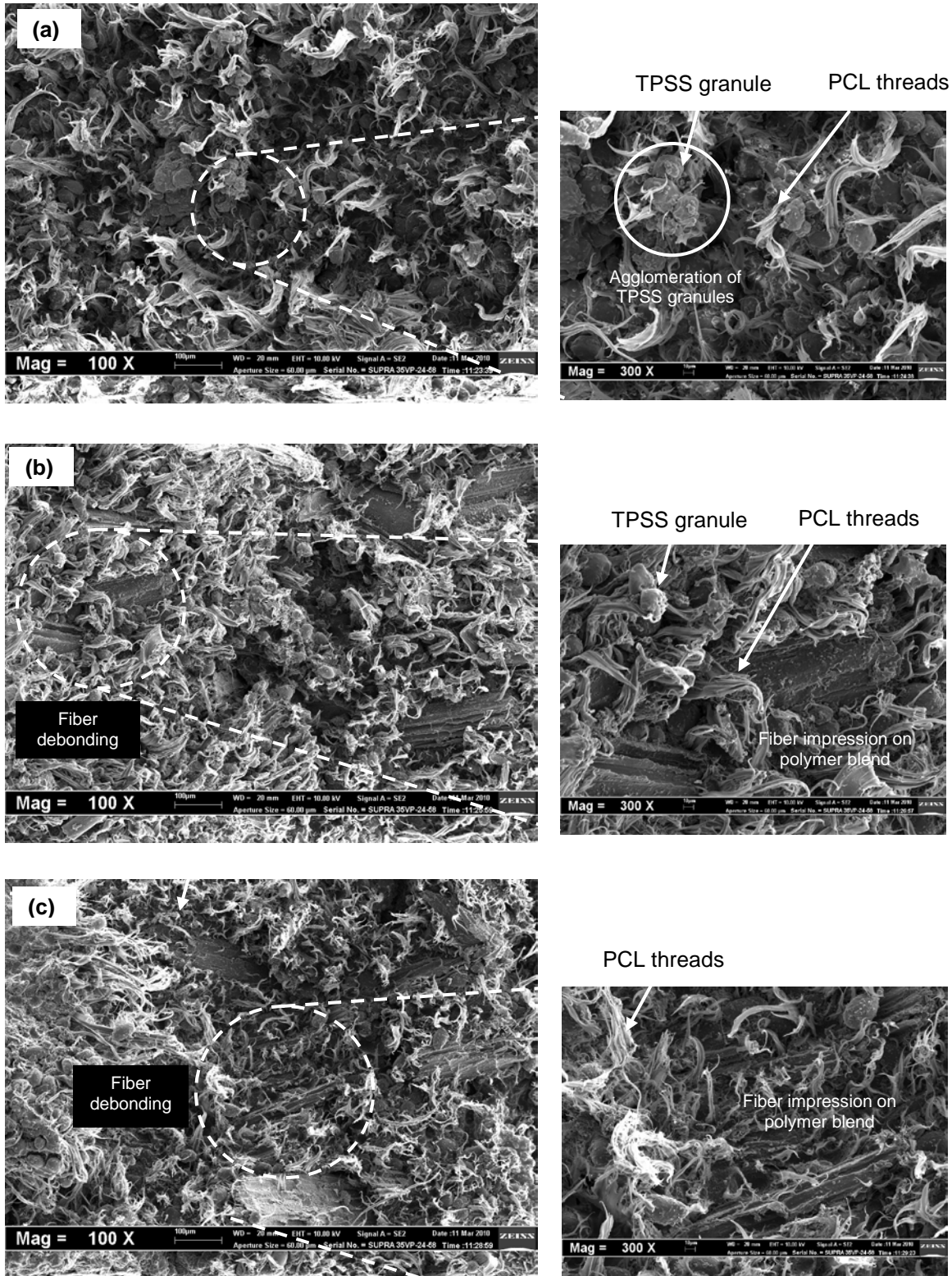
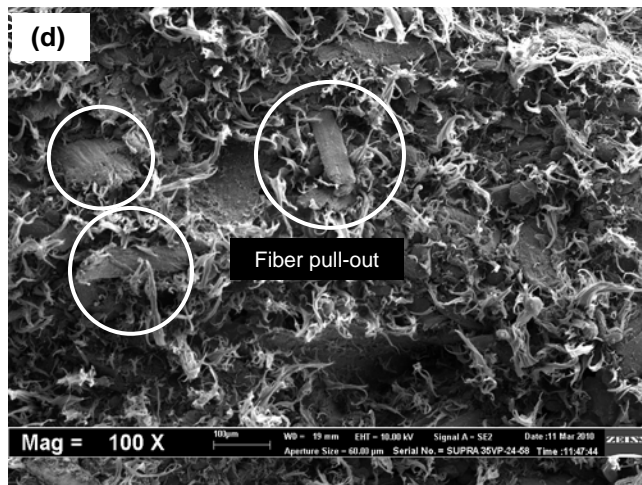


Fig. 10 (a-c). SEM micrographs on tensile fracture surfaces (see details on next page)



**Fig. 10.** SEM micrographs on tensile fracture surface of (a) PCL/TPSS blend (insert shows micrograph at higher magnification) and its biocomposites at (b) 5 phr (insert shows micrograph at higher magnification), (c) 10 phr (insert shows micrograph at higher magnification), and (d) 30 phr kenaf filler loading

The results are consistent with the fracture morphology of the untreated biocomposites. In Fig. 11 (b) and (c), which are referred to as PCL/TPSS/5KD and PCL/TPSS/10KD biocomposites, respectively, both systems exhibited almost similar features, i.e. KD impressions on polymer blend was observed at the fracture surface, suggesting that fiber debonding occurred and adhesion at fiber/matrix interface was poor. As for PCL/TPSS/30KD, Fig. 11 (d) illustrates fiber pull-out, which is not traceable in the fracture surfaces of PCL/TPSS/5KD and PCL/TPSS/10KD biocomposites. At high filler loading, it can be deduced that probability of longer length kenaf fibers presented in the biocomposite was higher and the orientation of some of these long fibers was aligned to the direction of applied force. As a result, the phenomenon of fiber pull-out was observed, which signifies higher strength of the biocomposite.

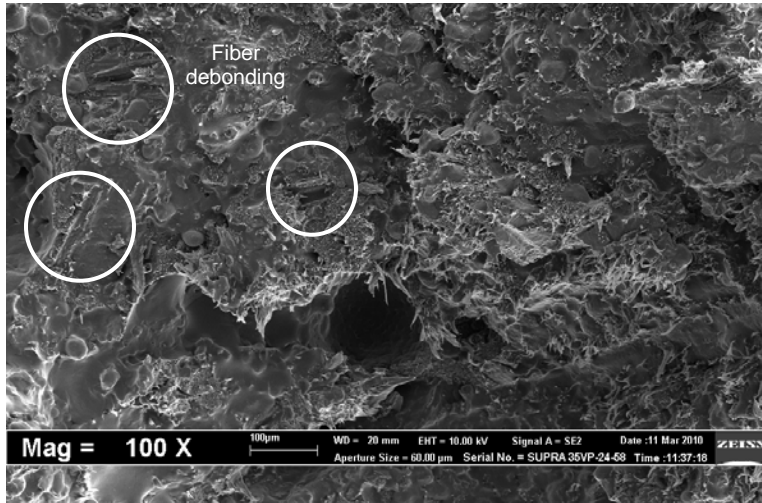
Meanwhile, the incorporation of KD improved the modulus of the PCL/TPSS blend significantly, as shown in Fig. 9 (b). The tensile modulus of the biocomposites was improved by more than fivefold at 30 phr filler content (1020 MPa) as compared to the PCL/TPSS blend (192 MPa), signifying that the presence of stiffer KD caused a decrease in mobility of the macromolecules of the matrix (Premalal et al. 2002; Pan et al. 2008). However, the elongation at break of the biocomposites showed a reverse trend whereby the increasing filler loading resulted in an abrupt drop in the elongation at break. PCL exhibits outstanding ductility in which its fracture surface usually appears fibrous due to stretching of its polymer threads (Correlo et al. 2005). Incorporation of TPSS reduced the ductility of the PCL as the amount of ductile PCL was reduced and agglomeration of TPSS granules into spherical domains acted as stress raisers during deformation of the polymer blend. In the case of composite, it is observed that an increase of filler loading further accompanies a decrease of polymer content available for elongation; thus decreases the elongation at break. This is in agreement with work done by Pan et al.

(2008) which highlighted that in the composite, all the elongation arises from the polymer. As far as the biocomposites are concerned, the tensile strength and modulus increased significantly with the filler content, while the elongation at break decreased. This evolution is characteristic of a reinforcing effect, which is classically observed for the reinforcement of polymer materials, with either synthetic or natural fibers (Kunanopparat et al. 2008).

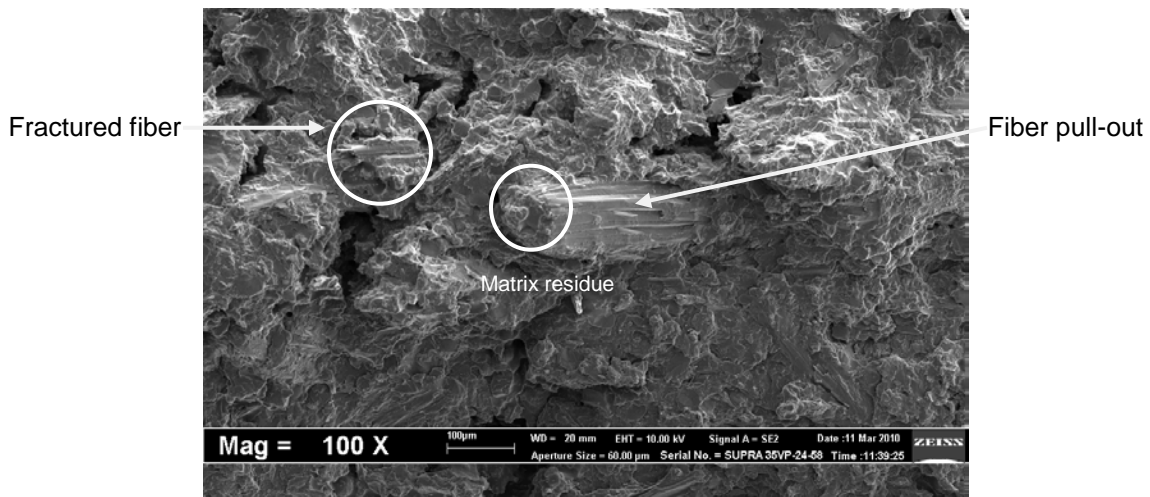
In terms of maleic anhydride treatment, like the control, as filler loading increased, the tensile strength and modulus of PCL-MAH/TPSS/KD biocomposites increased. Even so, it is noticeable that the biocomposites suffered an abrupt drop in the tensile strength relative to the untreated biocomposites at low filler loading (i.e. at 5 and 10 phr KD). The deterioration in the aforementioned properties is presumed to be a result of excessive concentration of DCP being incorporated into the PCL/TPSS blend during grafting polymerization. It is reported that polymer chain scission is very likely to occur when the concentration of DCP has exceeded its optimum level, causing increased amounts of short polymer chains (Mani et al. 1999). The tensile fracture surface of MAH-treated biocomposites with 10 phr KD content in Fig. 11 (a) further confirmed this phenomenon as fiber debonding is evident due to the poor adhesion between the short polymer chains and KD.

However, at a filler loading above 10 phr, the treated biocomposites were able to enhance the tensile properties in comparison to those of the untreated one. In this case, the increase of filler loading accompanies a decrease of polymer matrix content, and the concentration of DCP, which is held in constant proportion to the PCL/TPSS matrix content, was also reduced, and thus it is expected that the amount of filler loaded into the biocomposites has compensated for the undesirable effect of excess DCP concentration. For this, the effective coupling mechanism of MAH between the compatibilized polymer blend and kenaf can be attributed to esterification, as illustrated in Fig. 1 (b). The hydroxyl group of kenaf reacted with the anhydride group of MAH to form an ester linkage (Ganster et al. 2006; Li et al. 2007; Yang et al. 2007), as illustrated in Fig.1 (b). Consequently, the filler/matrix interfacial adhesion improves, causing the stress transferred from PCL/TPSS to the kenaf to be more effective and thus increasing the tensile strength of the biocomposites. At the same time, the modulus increases as the mobility of the macromolecules is restricted by the presence of the filler, leading to a stiffening effect. The tensile strength of the biocomposites increased by 19.7% and 41.4%, while the modulus improved by 18.9% and 15.4%, relative to the untreated biocomposites at 15 phr and 30 phr filler loading, respectively. The efficiency of the coupling was also demonstrated by the SEM micrographs of the tensile fracture surface of biocomposites with 30 phr KD content, as shown in Fig. 11 (b). Matrix residue was observed on the pull-out fiber, suggesting that filler/matrix interfacial adhesion was improved as a consequence of esterification. This is in accordance with Yang et al.'s work (2007), whereby the biocomposites treated with 4.5 phr MAH exhibited brittle fracture due to efficient stress propagation, and the fracture occurred not at the interface, but at the filler itself. This is characteristic of a composite with a compatibilizing agent that causes brittle deformation of the composite when tensile stress is applied (Yang et al. 2007). As for elongation at break, there is a general reduction trend as filler loading increased, as it is always the case, due to the reduced flexibility of PCL-MAH/TPSS,

except for PCL-MAH/TPSS/5KD biocomposites. However, compared with the equivalent biocomposites, the treated one showed higher elongation at break than the untreated one.



(a)



(b)

**Fig. 11.** SEM micrographs on tensile fracture surface of PCL-MAH/TPSS/KD biocomposites at (a) 10 phr and (b) 30 phr kenaf filler loading

## CONCLUSIONS

1. Incorporation of kenaf dust (KD) enhanced the tensile strength and modulus of the PCL/TPSS/KD biocomposites at the expense of elongation at break. The reinforcing effect imparted by KD was attributed to good dispersion of KD within the matrix, resulting in efficient stress transfer.

2. In maleic anhydride (MAH)-treated biocomposites, excessive DCP content caused reduction in relative strength at low kenaf filler loading. However, this interruption was not harmful to strength at high filler loading, as there was more filler to interact with the PCL-MAH/TPSS component.
3. In the water absorption behaviour, water uptake by the untreated biocomposites increased with the increase of kenaf filler loading because of the inherent hydrophilicity of KD as well as the possible presence of voids at the filler-matrix interface.
4. As for the treated biocomposites, a lower water uptake than the untreated one was observed and, in fact, a loss in weight was observed at low filler content, suggesting leaching out of starch and low molecular weight substances due to a high affinity to water molecules and inferior interfacial adhesion.

## ACKNOWLEDGMENTS

The authors are thankful to Universiti Teknikal Malaysia Melaka (UTeM) for the scholarship funded for support of the corresponding author in order to complete this work.

## REFERENCES CITED

- Abu-Sharkh, B. F., and Hamid, H. (2004). "Degradation study of date palm fiber/polypropylene composites in natural and artificial weathering: Mechanical and thermal analysis," *Polym. Degrad. Stabil.* 85(3), 967-973.
- Avella, M., Errico, M. E., Laurienzo, P., Martuscelli, E., Raimo, M., and Rimedio, R. (2000). "Preparation and characterization of compatibilised polycaprolactone/starch composites," *Polymer* 41(10), 3875-3881.
- Berkovich, L. A., Tsyurupa, M. P., and Davankov, V. A. (1983). "The synthesis of crosslinked copolymers of maleilated chitosan and acrylamide," *Journal of Polymer Science: Polymer Chemistry Edition* 21(5), 1281-1287.
- Bledzki, A. K., and Gassan, J. (1999). "Composites reinforced with cellulose based fibers," *Prog. Polym. Sci.* 24(2), 221-274.
- Bogoeva-Gaceva, G., Avella, M., Malinconico, M., Buzarovska, A., Grozdanov, A., Gentile, G., and Errico, M. E. (2007). "Natural fiber eco-composites," *Polym. Composite* 28(1), 98-107.
- Cyras, V. P., Martucci, J. F., Iannace, S., and Vazquez, A. (2002). "Influence of the fiber content and the processing conditions on the flexural creep behaviour of sisal-PCL-starch composites," *J. Thermoplast. Compos.* 15(3), 253-265.
- Correlo, V.M., Boesel, L.F., Bhattarcharya, M., Mano, J.F., Neves, N.M. and Reis, R. L. (2005). "Properties of melt processed chitosan and aliphatic polyester blends," *Mater. Sci. Eng. A* 403, 57-68.
- Demir, H., Atikler, U., Balköse, D., and Tihminlioğlu, F. (2006). "The effect of fiber surface treatments on the tensile and water sorption properties of polypropylene-luffa fiber composites," *Compos. Part A-Appl S.* 37(3), 447-456.

- Di Franco, C. R., Cyras, V. P., Busalmen, J. P., Ruseckaite, R. A., and Vázquez, A. (2004). "Degradation of polycaprolactone/starch blends and composites with sisal fiber," *Polym. Degrad. Stabil.* 86(1), 95-103.
- Ganster, J., Fink, H. P., and Pinnow, M. (2006). "High-tenacity man-made cellulose fiber reinforced thermoplastics - Injection molding compounds with polypropylene and alternative matrices," *Compos. Part A-Appl S.* 37(10), 1796-1804.
- George, J., Sreekala, M. S., and Thomas, S. (2001). "A review on interface modification and characterization of natural fiber reinforced plastic composites," *Polym. Eng. Sci.* 41(9), 1471-1485.
- Gross, R. A., and Kalra, B. (2002). "Biodegradable polymers for the environment," *Science* 297(5582), 803-307.
- Gáspár, M., Benkő, Zs., Dogossy, G., Réczey, K., and Czígány, T. (2005). "Reducing water absorption in compostable starch-based plastics," *Polym. Degrad. Stabil.* 90(3), 563-569.
- Hong, S. I., Choi, W. Y., Cho, S. Y., Jung, S. H., Shin, B. Y., and Park, H. J. (2009). "Mechanical properties and biodegradability of poly-ε-caprolactone/soy protein isolate blend compatibilized by coconut oil," *Polym. Degrad. Stabil.* 94(10), 1876-1881.
- Islam, T., Khan, R. A., Khan, M. A., Rahman, M. A., Fernandez-Lahore, M., Huque, Q.M.I., and Islam, R. (2009). "Physico-mechanical and degradation properties of gamma-irradiated biocomposites of jute fabric-reinforced poly(caprolactone)," *Polym.-Plast. Technol.* 48(11), 1198-1205.
- John, J., Tang, J., and Bhattacharya, M. (1998). "Processing of biodegradable blends of wheat gluten and modified polycaprolactone," *Polymer* 39(13), 2883-2895.
- John, J., Tang, J., Yang, Z. H., and Bhattacharya, M. (1997). "Synthesis and characterization of anhydride-functional polycaprolactone," *J. Polym. Sci. Pol. Chem.* 35(6), 1139-1148.
- Kim, H. S., Kim, H. J., Lee, J. W., and Choi, I. G. (2006). "Biodegradability of bio-flour filled biodegradable poly(butylenes succinate) bio-composites in natural and compost soil," *Polym. Degrad. Stabil.* 91(5), 1117-1127.
- Kunanopparat, T., Menut, P., Morel, M-H., and Guilbert, S. (2008). "Reinforcement of plasticized wheat gluten with natural fibers: From mechanical improvement to deplasticizing effect," *Compos. Part A-Appl S.* 39(5), 777-785.
- Lee, B. H., Kim, H. S., Lee, S. Kim, H. J., and Dorgan, J. R. (2009). "Bio-composites of kenaf fibers in polylactide: Role of improved interfacial adhesion in the carding process," *Compos. Sci. Technol.* 69(15-16), 2573-2579.
- Lei, Y., Wu, Q., Yao, F., and Xu, Y. (2007). "Preparation and properties of recycled HDPE/natural fiber composites," *Compos. Part A-Appl S.* 38(7), 1664-1674.
- Li, G., and Favis, B. D. (2010). "Morphology development and interfacial interactions in polycaprolactone/thermoplastic-starch blends," *Macromol. Chem. Physic* 211(3), 321-333.
- Li, X., Tabil, L. G., and Panigrahi, S. (2007). "Chemical treatments of natural fiber for use in natural fiber-reinforced composites: A review," *J. Polym. Environ.* 15(1), 25-33.

- Liu, W., Drzal, L. T., Mohanty, A. K., and Misra, M. (2007). "Influence of processing methods and fiber length on physical properties of kenaf fiber reinforced soy based biocomposites," *Compos. Part B-Eng* 38(3), 352-359.
- Liu, W., Misra, M., Askeland, P., Drzal, L. T., and Mohanty, A. K. (2005). "Green composites from soy based plastic and pineapple leaf fiber: Fabrication and properties evaluation," *Polymer* 46(8), 2710-2721.
- Mani, R., Bhattacharya, M., and Tang, J. (1999). "Functionalization of polyesters with maleic anhydride by reactive extrusion," *J. Polym. Sci. Pol. Chem.* 37(11), 1693-1702.
- Mohanty, A. K., Misra, M., and Drzal, L. T. (2005). *Natural Fibers, Biopolymers and Biocomposites*, CRC Press, Boca Raton, FL.
- Othman, N., Ismail, H., and Mariatti, M. (2006). "Effect of mechanical and thermal properties of bentonite filled polypropylene composites," *Polym. Degrad. Stabil.* 9198, 1761-1774.
- Pan, P., Zhu, B., Dong, T., Serizawa, S., Iji, M., and Inoue, Y. (2008). "Kenaf fiber/poly( $\epsilon$ -caprolactone) biocomposite with enhanced crystallization rate and mechanical properties," *J. Appl. Polym. Sci.* 107(6), 3512-3519.
- Premalal, H. G. B., Ismail, H., and Baharin, A. (2002). "Comparison of the mechanical properties of rice husk powder filled polypropylene composites with talc filled polypropylene composites," *Polym. Test.* 21(7), 833-839.
- Qiu, W., Endo, T., and Hirotsu, T. (2005). "A novel technique for preparing of maleic anhydride grafted polyolefins," *European Polymer Journal* 41(9), 1979-1984.
- Rahmat, A. R., Wan Abdul Rahman, W. A., Lee, T. S., and Yussuf, A. A. (2009). "Approaches to improve compatibility of starch filled polymer system: A review," *Mater. Sci. Eng. C* 29(8), 2370-2377.
- Ramarad, S. (2008). *Preparation and Properties of Kenaf Bast Fiber Filled (Plasticized) Poly(lactic acid) Composites*, MSc. Thesis, Penang: Universiti Sains Malaysia.
- Raquez, J. M., Nabar, Y., Srinivasan, M., Shin, B.Y., Narayan, R., and Dubois, P. (2008). "Maleated thermoplastic starch by reactive extrusion," *Carbohydr. Polym.* 74(2), 159-169.
- Rosa, D. S., Bardi, M. A. G., Machado, L. D. B., Dias, D. B., Silva, L. G. A., and Kodama, K. (2009). "Influence of thermoplastic starch plasticized with biodiesel glycerol on thermal properties of PP blends," *J. Therm. Anal. Calorim.* 97(2), 565-570.
- Rosa, D.S., Guedes, C.G.F., Pedroso, A.G. and Calil, M.R. (2004). "The influence of starch gelatinization on the rheological, thermal, and morphological properties of poly( $\epsilon$ -caprolactone) with corn starch blends," *Mater. Sci. Eng. C* 24, 663-670.
- Rosa, D. S., Lopes, D. R., and Calil, M. R. (2005). "Thermal properties and enzymatic degradation of blends of poly( $\epsilon$ -caprolactone) with starches," *Polym. Test.* 24(6), 756-761.
- Semba, T., Kitagawa, K., Ishiaku, U.S., and Hamada, H. (2006). "The effect of crosslinking on the mechanical properties of polylactic acid/polycaprolactone blends," *J. Appl. Polym. Sci.* 101(3), 1816-1825.
- Sen, A., and Bhattacharya, M. (2000). "Residual stresses and density gradient in injection molded starch/synthetic polymer blends," *Polymer* 41(26), 9177-9190.

- Shin, B.Y., Lee, S.I., Shin, Y.S., Balakrishnan, S., and Narayan, R. (2004). "Rheological, mechanical and biodegradation studies on blends of thermoplastic starch and polycaprolactone," *Polym. Eng. Sci.* 44(8), 1429-1438.
- Sreekala, M. S., Kumaran, M. G., Joseph, S., Jacob, M., and Thomas, S. (2000). "Oil palm fiber reinforced phenol formaldehyde composites: Influence of fiber surface modifications on the mechanical performance," *Appl. Compos. Mater.* 7(5-6), 295-329.
- Wu, C. S. (2003). "Physical properties and biodegradability of meleated polycaprolactone / starch composite," *Polym. Degrad. Stabil.* 80(1), 127-134.
- Yang, H. S., Kim, H. J., Park, H. J., Lee, B. J., and Hwang, T. S. (2007). "Effect of compatibilizing agents on rice-husk flour reinforced polypropylene composites," *Compos. Struct.* 77(1), 45-55.

Article submitted: July 13, 2011; Peer review completed: August 20, 2012; Revised version received and accepted: February 10, 2012; Published: February 13, 2012.